

Evolutionary Population Synthesis model with binary stars – Yunnan-II model

F. Zhang^{1,2}, Z. Han^{1,2} and L. Li^{1,2}

¹National Astronomical Observatories/Yunnan Observatory,
Chinese Academy of Sciences, Kunming, 650011, China

²Key Laboratory for the Structure and Evolution of Celestial Objects,
Chinese Academy of Sciences, Kunming, 650011, China
email: zhangfh@ynao.ac.cn

Abstract. By considering a modified version of the evolutionary population synthesis (EPS) model for stellar populations (SPs) comprising binary stars, the retrieved galaxy and HII-region parameters/properties differ from the case of neglecting binary stars. The retrieved age, stellar metallicity and mass of galaxies increase (e.g. ~ 0.2 dex when using spectral fitting algorithm), whilst the star formation rate decreases (~ 0.2 dex). The radiation fields from intermediate-age SPs with binary stars could be potentially important ionizing sources in HII regions. Under this possibility, the theoretical division between star forming galaxy and AGN on the diagnostic diagrams would move towards the up-right corner and the retrieved gaseous metallicity would decrease.

Our prediction for the birth rate of binary neutron stars in SPs ranges from 10^{-9} to $10^{-6} M_{\odot}^{-1} \text{ yr}^{-1}$ when the kick velocity is from 0 to 190 km s⁻¹.

Keywords. galaxies: stellar content, galaxies: fundamental parameters, galaxies: evolution, stars: neutron

1. Introduction

Observationally, binary stars have been found in many environments (Duchene & Kraus 2013): protostars, pre-main-sequence stars, young nearby associations, young massive star clusters (Sana *et al.* 2012), open clusters and Population II stars. Evolutionary population synthesis (EPS) models are a basic tool in studies of clusters and galaxies. So, we could not neglect the effect of binary stars in EPS model.

We have included the effect of binary stars in the Yunnan-II EPS model (Zhang *et al.* 2004, 2005, <http://www1.ynao.ac.cn/~zhangfh>), in which different evolutions of binary stars are obtained via the rapid binary star evolution (BSE) algorithms of Hurley *et al.* (2002). Since then, the model is constantly updated by improving the algorithm, using up-to-date initial distributions for stellar populations (SPs) and the latest BSE code. BPASS is another EPS model considering the effect of binary stars (Eldridge & Tout 2008, <http://bplass.auckland.ac.nz>). In this model, the evolutions of binary stars are obtained by using the detailed Cambridge stellar evolution code STARS and the mass of the primary star in a binary system is within $5 \leq M_1/M_{\odot} \leq 120$. Recently, Hernandez-Perez & Charlot (2013) also have considered the effect of binary stars in their EPS model. They also used the BSE algorithms of Hurley *et al.* (2002), the main difference from our model is the adoption of different initial distributions for SPs.

Using the Yunnan-II EPS model, we studied the effects of binary stars on the retrieved parameters/properties of galaxies and HII regions, on the theoretical classification line between star forming galaxy (SFG) and AGN on the diagnostic diagrams. We propose

that the radiation fields from intermediate-age (IMA) SPs with binary stars are in theory possible candidates for significant central ionizing sources (CISs) of classic HII regions. [Ma et al. \(2018\)](#) used the BPASS EPS model, in which the effect of binary stars are considered to explain the missing photon problem. [Hernandez-Perez & Charlot \(2014\)](#) used their EPS model to revisit the UV-upturn problem of elliptical galaxies.

Binary degenerated objects are important gravitational wave sources and relate to short γ -ray bursts. So binary stars have drawn more and more attention. We argue that the supernova (SN) kick velocity is a key factor in computing both the birth rate of binary neutron stars (BNSs) in SPs and the SPs' BNS birth rate.

2. Overview

First, we need to construct a SP comprising binary stars. Differing from single SP, which only needs initial mass function (IMF), the SP comprising binary stars needs the distributions of the initial primary- and secondary-star masses (M_1 , M_2), the separation/period (P) and the eccentricity (e). For the IMF for primaries, $\phi(M_1)$, we used the prescriptions of [Miller & Scalo \(1979\)](#); [Kroupa et al. \(2001\)](#); [Salpeter \(1955\)](#) and [Chabrier \(2003\)](#). For the initial secondary-star mass distribution, we used two cases: (i) M_1 and M_2 are uncorrelated, $\phi(M_2)$ is the same as $\phi(M_1)$; (ii) M_1 and M_2 are correlated, the mass-ratio distribution ($q = M_2/M_1$) is a uniform or thermal form. For separation/period (P) distribution, we used a combination of power-law and constant separation distributions. Under this case, the binary fraction with $P < 100$ yr is $\sim 50\%$. For the eccentricity (e) distribution, we used a uniform or constant ($e = 0$) distribution.

Key ingredients in Yunnan-II EPS model are the stellar evolution tracks, the spectral library and the initial distributions of binary stars as outlined above. To obtain the stellar evolution tracks, we used the BSE algorithms of [Hurley et al. \(2002\)](#). For spectral library, we used BaSeL semi-empirical stellar spectral library ([Lejeune et al. 1997, 1998](#)).

3. Results

3.1. Effects of binary stars

Based on age, we divide the effects of binary stars on the SPs' model results and retrieved parameters/properties of galaxies and HII regions into three parts. The comparisons presented below are between the Yunnan-II models for SPs with and without binary stars.

At all ages ($t \sim 10^{6-10.1}$ yr), the inclusion of binary stars makes the SPs' colours bluer and mass-to-light ratio in K-band (M/L_K) larger by a factor of 0.2 dex at each metallicity Z . The reason is that binary interactions can produce some hotter stars, for example, naked helium stars, blue stragglers and subdwarf B stars (sdBs). The effects on the retrieved parameters of galaxies are displayed in two aspects: age/stellar-metallicity and stellar-mass. (i) The inclusion of binary stars would make the retrieved age and stellar metallicity of galaxies larger, consistent with the fact that the colours become red when the age or metallicity increases. (ii) The larger SPs' (M/L_K) naturally leads to the larger retrieved galaxies' stellar mass.

At late ages ($t \sim 10^9$ yr), the inclusion of binary stars raises the UV flux (by $\sim 10^2$ times at wavelength $\lambda \sim 1300\text{\AA}$) at all metallicities (see panel A of Fig. 1). SdBs are the main reason for this flux increase. This result is consistent with the findings presented by [Han et al. \(2007\)](#) which have considered the presence of sdBs produced by binary evolution path to explain the UV-upturn phenomenon of elliptical galaxies.

At intermediate ages ($t \sim 10^{7-8}$ yr), the flux with $\lambda < 912\text{\AA}$ is raised by the inclusion of binary stars (by $\sim 10^5$ times at $\lambda \sim 300\text{\AA}$) at all metallicities (see panel B of Fig. 1). This effect is mainly caused by the naked helium stars, which temperature reaches up to 10^5K . We summarize our conclusions related to the parameters and properties of galaxies and HII regions below.

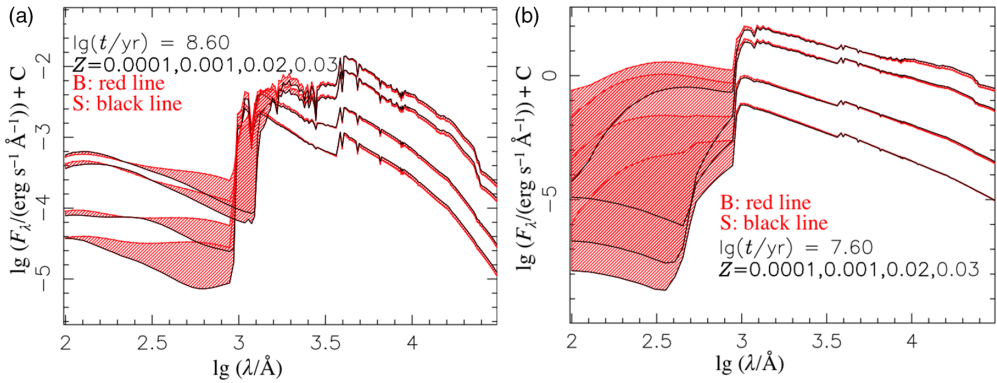


Figure 1. In each panel, ‘B’ and ‘S’ mean the cases considering binary stars and only single stars. The SPs’ ISEDs at $\lg(t/\text{yr}) = 8.6$ (panel A) and 7.6 (panel B).

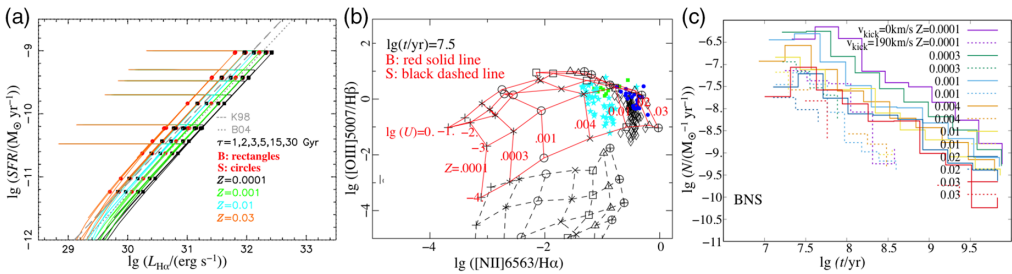


Figure 2. In each panel, ‘B’ and ‘S’ have the same meanings as in Fig. 1. (A) The relation between SFR and $L_{\text{H}\alpha}$ for E, S0, Sa-d galaxies (corresponding to $\tau = 1, 2, 3, 5, 15$ and 30 Gyr, from top to bottom), also shown are the results of K98 and B04. (B) Diagnostic diagram $\lg([\text{NII}]6563/\text{H}\alpha)$ versus $\lg([\text{OIII}]5007/\text{H}\beta)$ when the radiation fields from SPs with $\lg(t/\text{yr}) = 7.5$ are used as the CISs of HII regions and $\lg(U) = -4 \sim 0$, also shown are the observations of some spirals, dwarf-irregular galaxies and HII regions. (C) The BNS birth rate for SPs.

(i) *Star formation rate (SFR):* the luminosity of the H_α recombination line (L_{H_α}) is usually used to derive SFR. The inclusion of binary stars makes the galaxies’ model L_{H_α} larger at all metallicities (including E, S0, Sa-d galaxies, see panel A of Fig. 2), therefore making the retrieved SFR of galaxies smaller. For comparisons, we also plot the results of Kenicutt (1998, hereafter K98) and Brinchmann *et al.* (2004, hereafter B04). As the L_{H_α} increases with the number of ionizing photons $Q(\text{H})$, the inclusion of binary stars makes the flux with $\lambda < 912 \text{ \AA}$ larger and therefore $Q(\text{H})$ larger (Zhang *et al.* 2012).

(ii) *The CIS’ property of HII regions:* theoretical classification line between SFG and AGN on the diagnostic diagrams and gaseous metallicity of galaxies. In general, it is thought that the main CISs for classic H II regions are radiation fields emitted by O- and B-type stars or clusters of such stars. In the MAPPINGS photoionization code (Groves *et al.* 2008), we used the Yunnan-II EPS model results. When the radiation fields from IMA SPs with binary stars are used as the CISs of HII regions, we found the the model grid also can cover the regions occupied by spirals, dwarf-irregular galaxies and HII-regions (Zhang *et al.* 2015, and references therein) on the diagnostic diagrams. We concluded that the radiation fields from IMA SPs with binary stars can be in theory possible candidates for significant CISs of HII regions. The panel B of figure 2 presents our results for the predicted $\lg([\text{NII}]6563/\text{H}\alpha)$ versus $\lg([\text{OIII}]5007/\text{H}\beta)$ diagnostic diagram including binary stars. In the calculations, the hydrogen density n_{H} is fixed to 100 cm^{-3} while the ionization parameter ranges between $\lg(U) = -4$ and 0. With these assumptions, the theoretical classification line between SFG and AGN on the diagnostic

diagrams goes toward the up-right corner, the derived gaseous metallicity of galaxies would decrease (Zhang *et al.* 2015).

3.2. Birth rate of binary neutron stars

Binary stars are important gravitational wave sources and relate to short γ -ray bursts. Belczynski *et al.* (2018) predicted the BNS merger rate is $48 \text{ Gpc}^{-3} \text{ yr}^{-1}$, which is far less than LISA/Virgo prediction ($1540^{+3200}_{-1200} \text{ Gpc}^{-3} \text{ yr}^{-1}$, Abbott *et al.* 2017), so they concluded that the detection of GW170817 in NGC4993 is a statistical coincidence. After that, Chruslinska *et al.* (2018) used 19 sets of parameters and showed that their model prediction can reach to as high as $600^{+600}_{-300} \text{ Gpc}^{-3} \text{ yr}^{-1}$. We think that the main factor of affecting the BNS birth rate is the SN kick velocity V_{kick} . So we calculated the SPs' BNS birth rate as a function of time in the case of $V_{\text{kick}} = 0, 50$ and 190 km s^{-1} . The results are shown in panel C of Fig. 2 where we see that V_{kick} can largely affect the SPs' BNS birth rate by about two order of magnitudes between the cases of $V_{\text{kick}} = 0$ and 190 km s^{-1} (see Zhang *et al.* 2018 for details). Jiang *et al.* (2019) used our SPs' BNS birth rate results in the case of $V_{\text{kick}} = 50 \text{ km s}^{-1}$ in their semi-analytic model of galaxy evolution, obtaining a the BNS merger rate of $\sim 600 \text{ Gpc}^{-3} \text{ yr}^{-1}$ consistent with the finding of Chruslinska *et al.* (2018).

Acknowledgements

This work was funded by the Chinese Natural Science Foundation (grants 11573062, 11973081, 11773065, 11521303 and 11390734), the YIPACAS Foundation (grant 2012048) and the Yunnan Foundation (grant 2011CI053).

References

- Abbott, B., Abbott, R., Abbott, T., *et al.* 2017, *Phys. Rev. Lett.*, 119, 161101
 Belczynski, K., Askar, A., Arca-Sedda, M., *et al.* 2018, *A&A*, 615, A91
 Brinchmann, J., Charlot, S., White, S. D. M., *et al.* 2004, *MNRAS*, 351, 1151
 Chabrier, G. 2003, *PASP*, 115, 763
 Chruslinska, M., Belczynski, K., Klencki, J., Benacquista, M., *et al.* 2018, *MNRAS*, 474, 2937
 Duchene, G. & Kraus, A. 2013, *ARA&A*, 51, 269
 Eldridge, J. J., Izzard, R., & Tout, C. A. 2008, *MNRAS*, 384, 1109
 Kennicutt, R. C., Jr 1998, *ARA&A*, 36, 189
 Groves, B., Dopita, M., Sutherland, R., *et al.* 2008, *ApJS*, 176, 438
 Han, Z., Podsiadlowski, Ph., Lynas-Gray, A., *et al.* 2007, *MNRAS*, 380, 1098
 Hurley, J. R., Tout, C. A., & Pols, O. R. 2002, *MNRAS*, 329, 897
 Hernandez-Perez, F. & Charlot, G. 2013, *MNRAS*, 431, 2612
 Hernandez-Perez, F. & Charlot, G. 2014, *MNRAS*, 444, 2571
 Jiang, Z., Wang, J., *et al.* 2019, *in prep.*
 Kroupa, P., Aarseth, S., Hurley, J., *et al.* 2001, *MNRAS*, 321, 699
 Lejeune, T., Cuisinier, F., & Buser, R. 1997, *A&AS*, 125, 229
 Lejeune, T., Cuisinier, F., & Buser, R. 1998, *A&AS*, 130, 65
 Ma, X., Hopkins, P., Garrison-Kimmel, S., *et al.* 2018, *MNRAS*, 478, 1694
 Miller, G. E. & Scalo, J. M. 1979, *ApJS*, 41, 513
 Salpeter, E. E. 1955, *ApJ*, 121, 161
 Sana, H., de Mink, S. E., de Koteret, A., *et al.* 2012, *Sci.*, 444, 6
 Zhang, F., Han, Z., Li, L., Hurley, J., *et al.* 2004, *A&A*, 415, 117
 Zhang, F., Han, Z., Li, L., Hurley, J., *et al.* 2005, *MNRAS*, 357, 1088
 Zhang, F., Li, L., Zhang, Y., *et al.* 2012, *MNRAS*, 421, 743
 Zhang, F., Li, L., Han, Z., Kang, X., *et al.* 2015, *MNRAS*, 447, L21
 Zhang, F., Li, L., Han, Z., *et al.* 2018, *in prep.*